Structural Engineering and Mechanics, Vol. 8, No. 5 (1999) 513-529
DOI: http://dx.doi.org/10.12989/sem.1999.8.5.513

A posteriori error estimator for hierarchical models for elastic bodies with thin domain

Jin-Rae Cho †

School of Mechanical Engineering, Pusan National University, Pusan 609-735, Korea

Abstract. A concept of hierarchical modeling, the newest modeling technology, has been introduced in early 1990's. This new technology has a great potential to advance the capabilities of current computational mechanics. A first step to implement this concept is to construct hierarchical models, a family of mathematical models sequentially connected by a key parameter of the problem under consideration and have different levels in modeling accuracy, and to investigate characteristics in their numerical simulation aspects. Among representative model problems to explore this concept are elastic structures such as beam-, arch-, plate- and shell-like structures because the mechanical behavior through the thickness can be approximated with sequential accuracy by varying the order of thickness polynomials in the displacement or stress fields. But, in the numerical analysis of hierarchical models, two kinds of errors prevail, the modeling error and the numerical approximation error. To ensure numerical simulation quality, an accurate estimation of these two errors is definitely essential. Here, a local *a posteriori* error estimator for elastic structures with thin domain such as plate- and shell-like structures is derived using the element residuals and the flux balancing technique. This method guarantees upper bounds for the global error, and also provides accurate local error indicators for two types of errors, in the energy norm. Compared to the classical error estimators using the flux averaging technique, this shows considerably reliable and accurate effectivity indices. To illustrate the theoretical results and to verify the validity of the proposed error estimator, representative numerical examples are provided.

Key words: hierarchical model; elastic body; *a posteriori* error estimator; flux balancing; effectivity index.

1. Introduction

In every numerical analysis of natural phenomena using hierarchical models, at least two types of errors prevail; the error inherent in the hierarchical model itself due to assumptions made on it which may make it insufficient to depict significantly complicated features of the behavior, and the numerical error in the numerical approximation of the solution corresponding to a particular hierarchical model.

To the best of my memory, the mathematical derivation of *a priori* modeling error estimate for one-dimensional elliptic boundary value problems of scalar-valued functions was made by Vogelius and Babuska (1981). And recently, its extension to two- and three-dimensional linear elasticity problems with thin domain was done by the author and Oden (1996a). As for *a priori* error estimation of finite element approximations for elastic bodies with thin domain, the author and Oden (1996b) have presented the theoretical results reflecting the locking effect, and found

† Associate Professor

that two error components are orthogonal in the energy norm.

Schwab (1996) developed one simple *a posteriori* modeling error estimator for hierarchical models for plate-like structures using the decomposition of the modeling error and the use of traction residuals on the top and bottom surfaces of such structures.

This paper is concerned with a development of *a posteriori* error estimator which can accurately estimate the total error composed of the two error components, in other words, the error measured with respect to the fully three-dimensional linear elasticity theory. A reliable and efficient error estimator is an essential tool for selecting optimal hierarchical model and optimal finite element mesh.

Here, we use the mathematical theory advanced by Ainsworth and Oden (1993), which involves the use of localized element residuals and equilibrated flux-splitting to produce upper bounds for the global error in the energy norm. The implementation of this error estimator is composed of four steps: (1) We perform a finite element analysis with a setting of initial model (q_0) level and initial finite element mesh (h_0, p_0); (2) We then calculate equilibrated flux on each interelement boundary from the solutions obtained in step (1); (3) Next, we solve the local equilibrated problem for each element with higher model level q and higher approximation order p than those in the initial setting; (4) Finally we calculate local error indicators for each element using the two solutions obtained steps (1) and (3).

Error indicators estimated with this error estimator enable one to assess the validity of a specified hierarchical model as well as a specified finite element mesh for thin elastic bodies such as plate- and shell-like structures.

2. Preliminaries

Let Ω be an open *Lipschitzian* domain $\Re^3$ in with piecewise smooth boundary $\partial\Omega$. The spaces $H^m(\Omega)$ ($m \geq 0$, integers) are Hilbert spaces defined as the completion of $\{u \in C^m(\Omega) : \|u\|_{m,\Omega} < \infty\}$ in the Sobolev norm defined as

$$\| u \|_{m,\Omega} = \left\{ \sum_{|\alpha| \leq m} \int_\Omega | D^\alpha u |^2 d\Omega \right\}^{1/2} \tag{1}$$

where multi-index notation is used: $\alpha = (\alpha_1, \alpha_2, \alpha_3)$, $\alpha_i \geq 0$, $|\alpha| = \alpha_1 + \alpha_2 + \alpha_3$. Weak or distributional derivatives in the above equation are

$$D^\alpha u = \frac{\partial^{|\alpha|} u}{\partial x_1^{a_1} \partial x_2^{a_2} \partial x_3^{a_3}} \tag{2}$$

The inner product in the space $H^m(\Omega)$ is defined as

$$(u, v)_{m,\Omega} = \sum_{|\alpha|,|\beta| \leq m} \int_\Omega D^\alpha u \cdot D^\beta v d\Omega \tag{3}$$

Furthermore, $H_0^m(\Omega)$ is defined as the closure of $C_0^\infty(\Omega)$ in the space $H^m(\Omega)$. More mathematical details on the definition may be referred to Adams (1978).

Next, we introduce some useful notations concerning with the finite element partition, and which are used in the derivation of *a posteriori* error estimator. Let $\wp$ be a partition of Ω into a collection of $N = N(\wp)$ subdomains Ω_K with boundaries $\partial\Omega_K$ such that

i) $N(\wp) < \infty$
ii) Ω_K is *Lipschitzian* with piecewise smooth boundary $\partial\Omega_K$
iii) $\overline{\Omega} = \bigcup_{K=1}^{N} \overline{\Omega_K}$, $\Omega_K \cap \Omega_L = \emptyset$, $K \neq L$
iv) $\overline{\Omega_K} \cap \overline{\Omega_L}$ is either empty or common line or common smooth surface Γ_{KL}

Here, $\boldsymbol{n}_K$ is an outward unit vector normal on the boundary $\partial\Omega_K$, then $\boldsymbol{n}(s)$ on Γ_{KL} has

$$\begin{aligned} \boldsymbol{n}(s) &= \aleph_{KL}\, \boldsymbol{n}_K(s) = \aleph_{LK}\, \boldsymbol{n}_L(s) \\ \aleph_{KL} &= -\aleph_{LK} = \begin{cases} 1, & \text{if } K > L \\ -1, & \text{if } K < L \end{cases} \end{aligned} \tag{4}$$

and which implies $\boldsymbol{n}(s) = \boldsymbol{n}_K(s)$, $s \in \partial\Omega_K$ (K is a larger element number). In addition, we define the jump $[[v]]$ of functions v across the interelement boundary Γ_{KL} of two elements Ω_K and Ω_L by

$$[[v]] = \begin{cases} v_K - v_L, & \text{if } K > L \\ v_L - v_K, & \text{if } K < L \end{cases} \tag{5}$$

Futhermore, we denote k-th component of traction vector $\boldsymbol{t}$ of Cauchy stress tensor $\sigma(\boldsymbol{u})$ using the operator $\Gamma(\boldsymbol{n})$ containing the components of outward unit normal vector

$$t_k = \sigma_{kj} n_j = \langle \Gamma(\boldsymbol{n})\, \sigma(\boldsymbol{u}) \rangle^k \tag{6}$$

3. Formulation of hierarchical models

3.1 Variational formulation

For a purpose of notations, let us consider a plate-like structure with uniform thickness d, as shown in Fig. 1. Let $\omega \in \Re^2$ denote an open bounded region (mid-surface) of the body $\Omega \subset \Re^3$ with piecewise smooth boundary $\partial\omega$. We split the boundary $\partial\Omega_l$ into the lateral boundary and the top and bottom surfaces $\partial\Omega_\pm$ of the body, respectively

$$\begin{aligned} \partial\Omega_l &= \{\boldsymbol{x} \in \Re^3 \,|\, (x_1, x_2) \in \partial\omega,\ |x_3| < d/2\} \\ \partial\Omega_\pm &= \{\boldsymbol{x} \in \Re^3 \,|\, (x_1, x_2) \in \partial\omega,\ |x_3| = d/2\} \\ \partial\Omega_l &= \overline{\partial\Omega_l \cup \partial\Omega_\pm} \end{aligned} \tag{7}$$

Here, x_3 is a coordinate normal to the reference surface ω. Further, let Γ_D and Γ_N be the portions of the boundary $\partial\Omega$ such that $\overline{\Gamma_D \cup \Gamma_N} = \partial\Omega$, $\Gamma_D \cap \Gamma_N = \emptyset$, on which the displacements and the applied tractions are specified (i.e., Dirichlet and Neumann boundary regions), respectively. Usually, Γ_D is restricted to the lateral boundary and Γ_N to the top and bottom surfaces. For convenience of notations, we define $\partial\omega_D$, $\partial\omega_N$ by

$$\begin{aligned} \partial\Omega_D &\overset{def}{=} \Gamma_D|_\omega = \{\boldsymbol{x} \in \Gamma_D \,|\, x_3 = 0\} \\ \partial\omega_N &\overset{def}{=} \mathrm{Ptroj}_\omega(\Gamma_N) = \{(x_1, x_2, 0) \in \omega \,|\, (x_1, x_2, \pm d/2) \in \Gamma_N\} \end{aligned} \tag{8}$$

Viewing the structures as a three-dimensional elastic body (as opposed to abstract plates or shells), we have the following elliptic boundary value problems

$$-D^T \sigma(\boldsymbol{u}) = \boldsymbol{f}, \quad \text{in } \Omega$$

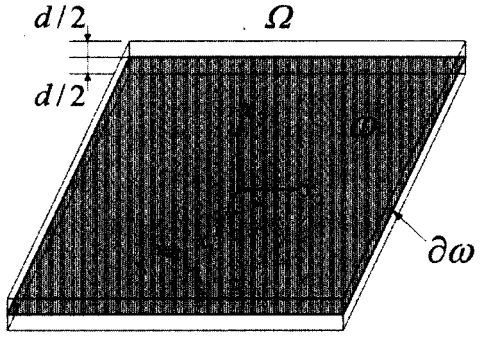

Fig. 1 A plate-like structure and its geometry notations

$$\begin{aligned} \boldsymbol{u} &= \boldsymbol{0}, \quad \text{on} \quad \Gamma_D \\ \Gamma(\boldsymbol{n})\,\sigma(\boldsymbol{u}) &= \boldsymbol{t}, \quad \text{on} \quad \Gamma_N \end{aligned} \tag{9}$$

and the strain-displacement relations and the constitutive equations

$$\begin{aligned} \varepsilon(\boldsymbol{u}) &= \boldsymbol{D}\,\boldsymbol{u} \\ \sigma(\boldsymbol{u}) &= \boldsymbol{E}\,\boldsymbol{D}\,\boldsymbol{u} \end{aligned} \tag{10}$$

Here, ε and σ are vectors of Cauchy strains and stresses, $\varepsilon=\{\varepsilon_1, \varepsilon_2, \varepsilon_3, \gamma_{12}, \gamma_{23}, \varepsilon_{31}\}^T$, $\{\sigma_1, \sigma_2, \sigma_3, \tau_{12}, \tau_{23}, \tau_{31}\}^T$ and $\boldsymbol{D}^T$denotes divergence-like operator in the Cartesian coordinate system

$$\boldsymbol{D}^T = \begin{bmatrix} \partial/\partial x_1 & 0 & 0 & \partial/\partial x_2 & 0 & \partial/\partial x_3 \\ 0 & \partial/\partial x_2 & 0 & \partial/\partial x_1 & \partial/\partial x_3 & 0 \\ 0 & 0 & \partial/\partial x_3 & 0 & \partial/\partial x_2 & \partial/\partial x_1 \end{bmatrix} \tag{11}$$

Here, $\boldsymbol{f}\in[L^2(\Omega)]^3$, $\boldsymbol{t}\in[L^2(\Omega)]^3$ represent body force and applied traction vectors, respectively. And $\boldsymbol{E}$ is a (6×6) matrix containing Lamé constants ν, λ for three-dimensional linear elastic materials (Szabo and Babuska 1991).

We define the space $V(\Omega)$ by $\{\boldsymbol{v}(x)\in[H^1(\Omega)]^3 : \boldsymbol{v}=\boldsymbol{0} \text{ on } \Gamma_D\}$, then this space is admissible displacement space for the elliptic boundary value problem (9) because every vector-valued function $\boldsymbol{v}\in V(\Omega)$ satisfies homogeneous boundary conditions on Γ_D and has finite strain energy $U(\boldsymbol{v})$. Now, let q be a set (q_1, q_2, q_3) with q_i of positive integers, and define the scalar-valued function space $V(\omega)$ defined on the mid-surface by

$$V(\omega)=\{v(x_1, x_2): v\in H^1(\omega)\,|\,\gamma_D\, v=0\} \tag{12}$$

where, $\gamma_D : H^1(\omega)\longrightarrow H^{1/2}(\partial\omega)$ is a trace operator. By introducing a set of Legendre polynomials $\Theta_l(x_3)$ and by specifying a set of their maximum orders (q_1, q_2, q_3), we define the subspace $V^q(\Omega)\subset V(\Omega)$ such that

$$V^q(\Omega)=\left\{ \boldsymbol{v}(x)\,|\,v_i=\sum_{l=0}^{q_i}\Theta_i^l(x_1, x_2)\circ\Psi_l(2x_3/d),\ \Theta_i^l\in V(\omega),\ i=1, 2, 3 \right\} \tag{13}$$

Then, from the density argument (Adams 1978), as $V_q(\Omega)\longrightarrow V(\Omega)$ as $q\longrightarrow\infty$.

The space $V^q(\Omega)$ is a restricted subspace of $V(\Omega)$ with finite dimension in the thickness variation in displacement fields. In this subspace, Galerkin weighed residual method for the three-dimensional linear elasticity leads to the weak statement:

$$\begin{aligned} &\text{Find } \boldsymbol{u}^q \in V^q(\Omega) \text{ such that } \forall\, \boldsymbol{v}^q \in V^q(\Omega) \\ &a(\boldsymbol{u}^q, \boldsymbol{v}^q) = l(\boldsymbol{v}^q) \end{aligned} \tag{14}$$

Where, the bilinear functional $a(\cdot, \cdot): V^q(\Omega) \times V^q(\Omega) \rightarrow \Re$ and the linear functional $l(\cdot): V^q(\Omega) \rightarrow \Re$ are expressed by the following dimensionally-reduced form defined on the mid-surface, respectively

$$\begin{aligned} a(\boldsymbol{u}^q, \boldsymbol{v}^q) &= \int_{-d/2}^{d/2} \langle (\boldsymbol{D}\, \boldsymbol{v}^q), (\boldsymbol{E}\boldsymbol{D}\boldsymbol{u}^q) \rangle_\omega dx_3 \\ l(v^q) &= \int_{-d/2}^{d/2} \langle \boldsymbol{f}, \boldsymbol{v}^q \rangle_\omega dx_3 + \langle \boldsymbol{t}^+, \boldsymbol{v}_q(\omega, d/2) \rangle_\omega + \langle \boldsymbol{t}^-, \boldsymbol{v}^q(\omega, -d/2) \rangle_\omega \end{aligned} \tag{15}$$

where, $\langle \cdot, \cdot \rangle$ is an inner product defined on the mid-surface domain by

$$\langle \boldsymbol{u}, \boldsymbol{v} \rangle = \int_\omega \boldsymbol{u}^T \boldsymbol{v}\, d\omega \tag{16}$$

Obviously, the variational problem (14) is two-dimensional because integrations through the thickness are related solely to the thickness polynomials $\psi_i(x_3)$.

The solution $\boldsymbol{u}^q$ of (14) is defined as a projection of $\boldsymbol{u}$ in the bilinear functional, $a(\boldsymbol{u}-\boldsymbol{u}^q, v) = 0$, $\forall v \in V^q(\Omega)$. We can construct a sequential set $\{\boldsymbol{u}^q\}_{q=1}^{\infty}$ of solution along the set of (q_1, q_2, q_3). We define the set of solutions as the **hierarchical family** F_H:

$$F_H = \{\boldsymbol{u}^q : q = 1, 2, \cdots, \infty\} \tag{17}$$

Hereafter, we will denote a hierarchical model with the model level (q_1, q_2, q_3) as **the** (q_1, q_2, q_3) **-model**. Their characteristics are well explained in the work of Babuska and Li (1992), Szabo and Babuska (1991), Cho and Oden (1996a, 1996b), Oden and Cho (1996) and Schwab (1996). We record here that the (q_1, q_2, q_3)*-models indicates the hierarchical models constructed by replacing $\boldsymbol{E}$ with $\boldsymbol{E}^{RM}$ of the Reissner-Mindlin theory.

3.2 Finite element approximation

Let us define the local function space V_K^q and the discontinuous global function space $V^q(\wp)$, respectively, by

$$\begin{aligned} V_K^q &= \{\hat{\boldsymbol{v}}_K^q : \hat{\boldsymbol{v}}_K^q \in [H^1(\Omega_K)]^3 \mid \hat{\boldsymbol{v}}_K^q = \boldsymbol{0} \text{ on } \partial\Omega \cap \Gamma_D\} \\ V^q(\wp) &= \prod_{K=1}^{N(\wp)} V_K^q \end{aligned} \tag{18}$$

then, $V^q(\Omega) \subset V^q(\wp)$. Hence, the global function $\hat{\boldsymbol{v}}^q \in V^q(\wp)$ is discontinuous at the interelement boundaries Γ_{KL} of subdomains Ω_K and Ω_L. Since the global finite element approximation $\boldsymbol{u}^{q,h}$ should be continuous at the interelement boundaries in order for finite strain energy, the global finite element approximation space $V^{q,h} \subset V^q$ should contain vector-valued test functions such that

$$V^{q,h} = \prod_{K=1}^{N(\wp)} V_K^q \cap [C^0(\overline{\Omega})]^3 \tag{19}$$

Then, the finite element approximation for the hierarchical model is as follows:

$$\begin{aligned} &\text{Find } \boldsymbol{u}^{q,h} \in V^{q,h}(\Omega) \text{ such that } \forall\, \boldsymbol{v}^{q,h} \in V^{q,h}(\Omega) \\ &a(\boldsymbol{u}^{q,h}, \boldsymbol{v}^{q,h}) = l(\boldsymbol{v}^{q,h}) \end{aligned} \tag{20}$$

Since the assumed admissible displacement fields are in the form of Eq. (13), finite element approximation is to find approximate solutions $\Theta_i^{l,h}(x_1, x_2)$ corresponding to each thickness-polynomial using two-dimensional finite-element basis functions $\{\varphi_k(x_1, x_2)$ such that

$$\Theta_i^{l,h}(x_1, x_2) = \sum_{k=1} \overline{\Theta}_{i,k}^{l,h} \circ \varphi_k(x_1, x_2) \tag{21}$$

Clearly, at each finite element node, $(q_1+q_2+q_3+3)$ degrees of freedom $\{\overline{\Theta}_{i,k}^{l,h}\}_{l=0}^{qi}$ are assigned.

4. *A posteriori* error estimation

4.1. Upper bound and local error indicators

Let $\boldsymbol{u}$ and $\boldsymbol{u}^q$ be the exact solutions of the three-dimensional elasticity and the hierarchical model with a model level $\boldsymbol{q}=\{q_1, q_2, q_3\}$, respectively. Then, the *modeling error* $\boldsymbol{e}^q \in V(\Omega)$ of the hierarchical model is defined as $\boldsymbol{e}^q = \boldsymbol{u} - \boldsymbol{u}^q$. And let $\boldsymbol{u}^{q,h}$ be the solution of the finite element approximation of the hierarchical model, then its finite element *approximation error* $\boldsymbol{e}^{q,h} \in V(\Omega)$ is denoted by $\boldsymbol{e}^{q,h} = \boldsymbol{u}^q - \boldsymbol{u}^{q,h}$. Combining these two errors, we define the finite element approximation error measured with respect to the exact solution

$$\boldsymbol{e} \in V(\Omega),\ \boldsymbol{e} = \boldsymbol{e}^q + \boldsymbol{e}^{q,h} = \boldsymbol{u} - \boldsymbol{u}^{q,h} \tag{22}$$

Here, we define the energy norm $\|\cdot\|_E$ in terms of the bilinear functional

$$\|\boldsymbol{v}\|_E = \sqrt{a(\boldsymbol{v}, \boldsymbol{v})} \tag{23}$$

And let the linear functionals $\Pi: V(\Omega) \rightarrow \Re$, $\Pi_q: V^q \rightarrow \Re$ and $J: V(\Omega) \rightarrow \Re$ be defined as, respectively

$$\begin{aligned} \Pi(\boldsymbol{v}) &= \frac{1}{2} a(\boldsymbol{v}, \boldsymbol{v}) - l(\boldsymbol{v}) \\ \Pi_q(\boldsymbol{v}) &= \frac{1}{2} a(\boldsymbol{v}^q, \boldsymbol{v}^q) - l(\boldsymbol{v}^q) \\ J(\boldsymbol{v}) &= \Pi(\boldsymbol{v}) - \Pi_q(\boldsymbol{u}^{q,h}) \end{aligned} \tag{24}$$

Then, the difference between the two potential functionals $\Pi(\boldsymbol{u})$ and $\Pi_q(\boldsymbol{u}^{q,h})$ is expressed by

$$\begin{aligned} J(\boldsymbol{u}) &= \frac{1}{2} a(\boldsymbol{u}, \boldsymbol{u}) - l(\boldsymbol{u}) - \frac{1}{2} a(\boldsymbol{u}^{q,h}, \boldsymbol{u}^{q,h}) + l(\boldsymbol{u}^{q,h}) \\ &= \frac{1}{2} a(\boldsymbol{u} - \boldsymbol{u}^{q,h}, \boldsymbol{u} - \boldsymbol{u}^{q,h}) - l(\boldsymbol{u}) + l(\boldsymbol{u}^{q,h}) + a(\boldsymbol{u}, \boldsymbol{u}) - a(\boldsymbol{u}, \boldsymbol{u}^{q,h}) \end{aligned} \tag{25}$$

where we use the fact that $a(\boldsymbol{u}^{q,h}, \boldsymbol{u}^{q,h})$ and $l(\boldsymbol{u}^{q,h})$ are restrictions from the space V into V^q, respectively. It is not difficult to prove

$$\frac{1}{2} \|\boldsymbol{e}\|_E^2 = J(\boldsymbol{u}) = \Pi(\boldsymbol{u}) - \Pi_q(\boldsymbol{u}^{q,h})$$

$$= \inf_{v \in V(\Omega)} \Pi(v) - \Pi_q(u^{q,h}) \tag{26}$$

We next define the local solution spaces V_K in a subdomain Ω_K, and the broken space $V(\wp)$

$$V_K = \{v \in [H^1(\Omega_K)]^3 \,|\, v = 0 \text{ on } \partial\Omega_K \cap \Gamma_D\} \tag{27}$$

$$V(\wp) = \prod_{K=1}^{N(\wp)} V_K, \quad V(\wp) \supset V(\Omega) \tag{28}$$

then, $v \in V(\wp)$ and $V^q(\wp)$ are discontinuous across the interelement boundary Γ_{KL}. In the local spaces V_K, V_K^q the bilinear and the linear functionals $a(\cdot, \cdot)$ $l(\cdot)$ and Π restricted to a finite element are denoted by $a_K(\cdot, \cdot)$ $l_K(\cdot)$ and Π_K, respectively.

With the splitting function $\alpha_{KL} : \Gamma_{KL}(s) \longrightarrow \Re$ defined on the interelement boundary $\Gamma_{KL}(s)$ as

$$\alpha_{KL}^k(s) + \alpha_{LK}^k(s) = 1, \quad k = 1, 2, 3 \tag{29}$$

we define k-th component of the self-equilibrated traction acting on the element Ω_K along $\Gamma_{KL}(s)$ as

$$\langle \Gamma(n)\sigma(u^{q,h})\rangle_{1-\alpha}^k = \alpha_{LK}^k \langle \Gamma(n_K)\sigma(u_K^{q,h})\rangle^k + \alpha_{KL}^k \langle \Gamma(n_K)\sigma(u_L^{q,h})\rangle^k \tag{30}$$

then, for every $v \in V^q(\wp)$

$$\sum_{K=1}^{N(\wp)} \int_{\partial\Omega_K/\partial\Omega} v^T \langle \Gamma(n)\sigma(u^{q,h})\rangle_{1-\alpha}\, ds = \sum_{\Gamma_{KL}} \int_{\Gamma_{KL}} [[v^T]] \langle \Gamma(n)\sigma(u^{q,h})\rangle_{1-\alpha}\, ds \tag{31}$$

Next, we extend Π to the spaces $V(\wp)$ and $V^q(\wp)$, respectively, and consider the difference functional (potential functional) $J_\wp : V(\wp) \longrightarrow \Re$ expressed by

$$\begin{aligned} J_\wp(v) &= \Pi(v) - \Pi(u^{q,h}), \quad v \in V(\wp) \\ &= \sum_{K=1}^{N(\wp)} \left\{ \Pi_K(v) - \Pi_K(u^{q,h}) - \int_{\partial\Omega_K/\partial\Omega} v^T \langle \Gamma(n)\sigma(u^{q,h})\rangle_{1-\alpha}\, ds \right\} \\ &\quad + \sum_{\Gamma_{KL}} \int_{\Gamma_{KL}} [[v^T]] \langle \Gamma(n)\sigma(u^{q,h})\rangle_{1-\alpha}\, ds \end{aligned} \tag{32}$$

We ensure that the interelement jumps $[[v]]$ are constrained to be zero by using a Lagrange multiplier μ, and that leads to a introduction of the Lagrange functional Λ defined by

$$\begin{aligned} &\Lambda : V(\wp) \times \Xi \to \Re \\ &\Lambda(v, \mu) = J_\wp(v) - \mu([[v]]) \end{aligned} \tag{33}$$

where, the Ξ denotes the space of Lagrange multipliers. From Eqs. (32) and (33), we get

$$\begin{aligned} \Lambda(v, \mu) = &\sum_{K=1}^{N(\wp)} \left\{ \Pi_K(v) - \Pi_K(u^{q,h}) - \int_{\partial\Omega_K/\partial\Omega} v^T \langle \Gamma(n)\sigma(u^{q,h})\rangle_{1-\alpha}\, ds \right\} \\ &- \mu([[v]]) + \sum_{\Gamma_{KL}} \int_{\Gamma_{KL}} [[v^T]] \langle \Gamma(n)\sigma(u^{q,h})\rangle_{1-\alpha}\, ds \end{aligned} \tag{34}$$

This functional is composed of sum of local contributions from each element Ω_K and extra coupled terms from each interelement boundary Γ_{KL}. But, if we take $\mu = \hat{\mu}$, then Λ becomes a sum of purely uncoupled local contributions

$$\hat{\mu}([[\nu]]) = \sum_{\Gamma_{KL}} \int_{\Gamma_{KL}} [[\nu^T]] \langle \Gamma(\boldsymbol{n}) \Gamma(\boldsymbol{u}^{q,h}) \rangle_{1-\alpha} \, ds \tag{35}$$

Using the relation (31), we note that, for any $\nu \in V(\Omega)$, $\Lambda(\nu, \mu) = J(\nu)$ and from Eq. (26), we have

$$-\frac{1}{2} \| e \|_E^2 = J(\boldsymbol{u}) = \inf_{\nu \in V(\Omega)} \Lambda(\nu, \mu) \tag{36}$$

Now, let us define the functional $\Phi: V(\wp) \longrightarrow \overline{\Re}$ as $\Phi(\nu) = \sup_{\mu \in \Xi} \Lambda(\nu, \mu)$, then it shows

$$\Phi(\nu) = \begin{cases} J(\nu), & \nu \in V(\Omega) \\ +\infty & \nu \notin V(\Omega) \end{cases} \tag{37}$$

and $\inf_{\nu \in V(\wp)} \Phi(\nu) = \inf_{\nu \in V(\Omega)} \Phi(\nu) = 2\|e\|_E^2$. Moreover, the next relation holds :

$$\begin{aligned} \inf_{\nu \in V(\Omega)} J(\nu) &= \inf_{\nu \in V(\wp)} \sup_{\mu \in \Xi} \Lambda(\nu, \mu) \\ &\geq \sup_{\mu \in \Xi} \inf_{\nu \in V(\wp)} \Lambda(\nu, \mu) \\ &\geq \inf_{\nu \in V(\wp)} \Lambda(\nu, \hat{\mu}), \quad \forall \, \hat{\mu} \in \Xi \end{aligned} \tag{38}$$

With the choice of a Lagrange multiplier $\hat{\mu}$ in Eq. (35), an upper bound of the global error is expressed by

$$\| e \|_E^2 \leq -2 \sum_{K=1}^{N(\wp)} \inf_{\nu \in V_K} \left\{ \Pi_K(\nu) - \Pi_K(\boldsymbol{u}^{q,h}) - \int_{\partial\Omega_K / \partial\Omega} \nu^T \langle \Gamma(\boldsymbol{n}_K) \sigma(\boldsymbol{u}^{q,h}) \rangle_{1-\alpha} \, ds \right\} \tag{39}$$

Since the second term in RHS of Eq. (39) computed from the finite element approximate solution $\boldsymbol{u}^{q,h}$ is invariant, we need only to solve the following local element-wise variational problems :

$$\begin{aligned} &\text{Find } \hat{\boldsymbol{u}}_K \in V_K \text{ such that } \forall \nu \in V_K \\ &a_K(\hat{\boldsymbol{u}}_K, \nu) = l_K(\nu) + \int_{\partial\Omega_K / \partial\Omega} \nu^T \langle \Gamma(\boldsymbol{n}_K) \sigma(\boldsymbol{u}^{q,h}) \rangle_{1-\alpha} \, ds \end{aligned} \tag{40}$$

Obviously, the equilibrated local problems are defined on three-dimensional broken spaces V_K. With this $\hat{\boldsymbol{u}}_K$, Eq. (39) becomes

$$\begin{aligned} &-2 \inf_{\nu \in V_K} \left\{ \Pi_K(\nu) - \Pi_K(\boldsymbol{u}^{q,h}) - \int_{\partial\Omega_K / \partial\Omega} \nu^T \langle \Gamma(\boldsymbol{n}_K) \sigma(\boldsymbol{u}^{q,h}) \rangle_{1-\alpha} \, ds \right\} \\ &\quad = a_K(\hat{\boldsymbol{u}}_K \hat{\boldsymbol{u}}_K) + 2\Pi_K(\boldsymbol{u}^{q,h}) \\ &\quad = a_K(\hat{\boldsymbol{u}}_K - \boldsymbol{u}^{q,h}, \hat{\boldsymbol{u}}_K - \boldsymbol{u}^{q,h}) + \int_{\partial\Omega_K / \partial\Omega} \boldsymbol{u}^{q,h^T} \langle \Gamma(\boldsymbol{n}_K) \sigma(\boldsymbol{u}^{q,h}) \rangle_{1-\alpha} \, ds \end{aligned} \tag{41}$$

and from the fact of $[[\boldsymbol{u}^{q,h}]] = \boldsymbol{0}$, Eq. (41) results in :

$$\begin{aligned} \| e \|_E^2 &\leq a_K(\hat{\boldsymbol{u}}_K - \boldsymbol{u}^{q,h}, \hat{\boldsymbol{u}}_K - \boldsymbol{u}^{q,h}) + \sum_{K>L}^{N(\wp)} \int_{\Gamma_{KL}} [[\boldsymbol{u}^{q,h^T}]] \langle \Gamma(\boldsymbol{n}_K) \sigma(\boldsymbol{u}^{q,h}) \rangle_{1-\alpha} \, ds \\ &= a_K(\hat{\boldsymbol{u}}_K - \boldsymbol{u}^{q,h}, \hat{\boldsymbol{u}}_K - \boldsymbol{u}^{q,h}) \end{aligned} \tag{42}$$

By denoting $a_K(\hat{\boldsymbol{u}}_K - \boldsymbol{u}^{q,h}, \hat{\boldsymbol{u}}_K - \boldsymbol{u}^{q,h})$ as $(\eta_K)^2$, we finally have

$$\| e \|_E^2 \leq \sum_{K=1}^{N(\wp)} (\eta_K)^2 \tag{43}$$

The quantity η_K is thus error indicator for element Ω_K and contributes to the global error bound.

Next, consider the discretization of the local element-wise problem (40) by introducing the local finite element approximation solution space $V_K^h = V_{pk*}^{pK*}(\Omega_K)$ as a restriction of the initial finite element approximation space $V^{q,h}(\Omega)$ in Eq. (19) to the element Ω_K with higher $p_K^* = p_K + \delta_p$ and $p_K^* = p_K + \delta_q$. Then, the corresponding discrete local element-wise problem is:

$$\text{Find } \hat{\boldsymbol{u}}_K^h \in V_K^h \text{ such that } \forall\, \boldsymbol{v}h \in V_K^h$$
$$a_K(\hat{\boldsymbol{u}}_K^h, \boldsymbol{v}^h) = l_K(\boldsymbol{v}^h) + \int_{\partial\Omega_K/\partial\Omega} \boldsymbol{v}^T \langle \Gamma(\boldsymbol{n}_K)\sigma(\boldsymbol{u}^{q,h})\rangle_{1-\alpha}\, ds \tag{44}$$

And then, $(\eta_K^h)^2 = a_K(\hat{\boldsymbol{u}}_K^h - \boldsymbol{u}^{q,h}, \hat{\boldsymbol{u}}_K^h - \boldsymbol{u}^{q,h}) \approx (\eta_K)^2$.

4.2. Calculation of self-equilibrating fluxes

Here, we introduce the local flux-splitting and equilibration method proposed by Ainsworth and Oden (1993). Finite element approximations of hierarchical models are two-dimensional, but the flux- splitting on the interelement boundaries is three-dimensional. Let $F(\wp)$ denote the set of all vertices in the partition, and consider any vertex $A \in F(\wp)$. Associated with each such vertex node A is a piecewise tri-linear shape function $\varphi_A(\boldsymbol{x})$, which vanishes at every other vertex node in this partition and has a unit value at the node A. With this shape function, the flux splitting function $\alpha_{KL}(\boldsymbol{s})$ of Eq. (29) is expressed on the interelement face Γ_{KL} with four end nodes, A, B, C and D, by

$$\alpha_{KL}^k(\boldsymbol{s}) = \sum_{N=A}^{D} \alpha_{KL}^k(\boldsymbol{s})\varphi_N(\boldsymbol{s}),\ k = 1, 2, 3 \tag{45}$$

Now, return to the local weak formulation for a single element $\Omega_K \in N(\wp)$ with a sufficiently smooth vector-valued test function $\boldsymbol{\phi}(\boldsymbol{x})$. If we take $\boldsymbol{\phi} = (1, 1, 1)^T$, then

$$a_K(\boldsymbol{u}, 1) = l_K(1) + \int_{\partial\Omega_K/\partial\Omega} 1^T \Gamma(\boldsymbol{n})\sigma(\boldsymbol{u})\, ds \tag{46}$$

The above equation characterizes the equilibration of an element Ω_k, and its solution $\boldsymbol{u}|_{\Omega K}$ is the restriction of true solution $\boldsymbol{u}$ to the element Ω_K. If we replace $\boldsymbol{u}$ in Eq. (46) with the initial finite element approximate solution $\boldsymbol{u}^{q,h}$ and rewrite the above equation for each component of the test function $\mathbf{1} = \mathbf{1}^1 + \mathbf{1}^2 + \mathbf{1}^3 = \{(1, 0, 0) + (0, 1, 0) + (0, 0, 1)\}^T$. Then Eq. (47) represents the compatibility condition for the kth interelement traction component for $< \cdot >_{1-\alpha}^k$ the existence of local solution :

$$a_K(\boldsymbol{u}^{q,h}, \mathbf{1}^k) = l_K(\mathbf{1}^k) + \int_{\partial\Omega_K/\partial\Omega} \langle \Gamma(\boldsymbol{n})\sigma(\boldsymbol{u}^{q,h})\rangle_{1-\alpha}^k\, ds \tag{47}$$

Since $\boldsymbol{u}^{q,h}$ is given from the initial finite approximation, compatibility condition implies to find splitting factors α_{KL}^k for the self-equilibrated traction component which make the element Ω_K be in force equilibrium in the kth direction.

The difference, RHS-LHS in Eq. (47), means the lack in the force equilibrium in the kth direction on Ω_K, here we denote it by Δ_K^k. Because the trilinear shape function $\varphi_A(\boldsymbol{x})$ has the following property,

$$\sum_{A \in F(\wp)} \boldsymbol{\varphi}_A^1(x) = (1, 0, 0)^T, \quad \forall \boldsymbol{x} = \Omega \tag{48}$$

the lack Δ_K^k of force equilibrium in the k-th direction is expressed by

$$\begin{aligned} \Delta_K^k &= \sum_{A \in F(\wp)} \Delta_{K,A}^k \\ \Delta_{K,A}^k &= l_k(\varphi_A^k) + \int_{\partial\Omega_K/\partial\Omega} (\varphi_A^k) \langle \Gamma(\boldsymbol{n}) \sigma(\boldsymbol{u}^{q,h}) \rangle_{1-\alpha}^k \, ds \\ &\quad - a_K(\boldsymbol{u}^{q,h}, \boldsymbol{\varphi}_A^k) \end{aligned} \tag{49}$$

The above equation has the significant importance that the coupled flux-splitting problem between elements in the patch $F(\wp)$ of the node A becomes the uncoupled problem for each node A.

For convenience of computation, we introduce an anti-symmetric operator $\kappa_{KL} : \Gamma_{KL} \longrightarrow \Re$

$$\kappa_{KL}^k = \alpha_{KL}^k - 1/2 \Rightarrow \kappa_{KL}^k + \kappa_{LK}^k = 0 \tag{50}$$

then, from Eqs. (30) and (50), we have

$$\begin{aligned} \langle \Gamma(\boldsymbol{n}) \sigma(\boldsymbol{u}^{q,h}) \rangle_{1-\alpha}^k &= \frac{1}{2} \langle \Gamma(\boldsymbol{n}) \sigma(\boldsymbol{u}_K^{q,h}) + \Gamma(\boldsymbol{n}) \sigma(\boldsymbol{u}_L^{q,h}) \rangle^k \\ &= \langle \Gamma(\boldsymbol{n}) \sigma(\boldsymbol{u}^{q,h}) \rangle_{1/2}^k + \kappa_{KL}^k [[\Gamma(\boldsymbol{n}) \sigma(\boldsymbol{u}^{q,h})]]^k \end{aligned} \tag{51}$$

With two quantities defined by

$$\begin{aligned} b_{K,A}^k &= l_k(\varphi_A^k) + \int_{\partial\Omega_K/\partial\Omega} (\varphi_A^k) \langle \Gamma(\boldsymbol{n}) \sigma(\boldsymbol{u}^{q,h}) \rangle_{1/2}^k \, ds - a_K(\boldsymbol{u}^{q,h}, \varphi_A^k) \\ \rho_{LK,A}^k &= -\int_{\Gamma_{KL}} \varphi_A^k [[\Gamma(\boldsymbol{n}) \sigma(\boldsymbol{u}^{q,h})]]^k \, ds \end{aligned} \tag{52}$$

Eq. (49) becomes

$$\begin{aligned} \Delta_{K,A}^k &= b_{K,A}^k - \sum_{L>0} \kappa_{LK,A}^k \rho_{LK,A}^k \\ &= b_{K,A}^k - \sum_{L>0} \hat{\kappa}_{LK,A}^k \end{aligned} \tag{53}$$

Then, $\hat{\kappa}_{LK}^k = -\hat{\kappa}_{KL}^k$ because κ_{LK}^k is anti-symmetric and $\rho_{LK,A}^k$ is symmetric. We will use $\hat{\kappa}_{LK}^k$ for $L > K$, then the vanishing of $\Delta_{K,L}^k$ is equivalent to

$$\sum_{L>K>0} \hat{\kappa}_{LK}^k - \sum_{K>L>0} \hat{\kappa}_{KL}^k = b_{K,A}^k \tag{54}$$

Now, consider a patch of elements sharing the common node A denoted by

$$\Im_A = \{ \cup \Omega_K \subset \Omega | \, \Omega_K \qquad \text{supp } (\varphi_A) \} \tag{55}$$

and, we construct a system of equations involving the elements in the patch of the node A. We finally compute the flux-splitting functions $\hat{\kappa}_{LK}^k$ on the interelement boundaries for each node by solving the following linear equations

$$\boldsymbol{M}_A \hat{\kappa}_A^k = \boldsymbol{b}_A^k, \; k = 1, 2, 3, \quad \forall A \in F(\wp) \tag{56}$$

where

$$\boldsymbol{b}_A^k = \{b_{K_1,A}^k, b_{K_1,A}^k \ldots, b_{K_{Aed},A}^k\}^T$$
$$\hat{\kappa}_A^k = \{\hat{\kappa}_{LK}^k, \ldots\}^T, \; L > K \tag{57}$$

Here, $\boldsymbol{M}_A$ is a $(N_{Aed} \times A_{Aed})$ underlying matrix for a patch consisting of N_{Aed} elements and N_{Aed} interelement faces sharing common node A.

After solving the linear system of equations, we compute the splitting factors α_{KL}^k with the relation (50), and calculate self-equilibrated tractions $< \cdot >_{1-\alpha}$ on interelement boundaries. With the computed self-equilibrated tractions, we finally solve the local approximation problems (44) to get better approximate solutions $\hat{\boldsymbol{u}}_K^h$ so that we estimate the error indicators.

5. Numerical experiments

Fig. 2 shows a clamped square plate-like body with uniform thickness. Uniformly distributed traction t_z is applied on the top surface. From the symmetry, only a quarter of the body is taken for numerical analysis. Data used for the analysis are $E = 10^7\,\mathrm{N/m^2}$, $\nu = 0.3$, $a = 1.0\,\mathrm{m}$ and $t_z = 5.0 \times 10^{-4}\,\mathrm{N/m^2}$. We use the (1,1,0)*-hierarchical model and 9 uniform quadratic elements. The distribution of vertical displacement component is shown in Fig. 3, where "DOM" refers to the ratio (or called the bending dominance) of bending strain energy to the total strain energy calculated from the approximated solution. The finite element simulation was carried out with the *Adaptive hpq-Finite Element CODE** which is fully automatic program capable of systematic selection of the optimal model and the optimal finite element mesh satisfying the predefined analysis tolerance.

In order to evaluate the quality of the proposed error estimator, the effectivity index θ is computed. Since the analytic solution for this problem is not available, we use the approximated solution $\boldsymbol{u}_{\mathrm{ref}}$ obtained with relatively higher model and higher approximation order but with the same mesh partition (here, we use q=(8, 8, 8) and p=8). With this alternative choice, we compute the local and global effectivity indices θ_K, θ defined by

$$\theta_k = \eta_K^k / \eta_K \approx \| \hat{\boldsymbol{u}}_K^h - \boldsymbol{u}^{q,h} \|_{E(\Omega_K)} / \| \boldsymbol{u}_{\mathrm{ref}} - \boldsymbol{u}^{q,h} \|_{E(\Omega_K)} \tag{58}$$

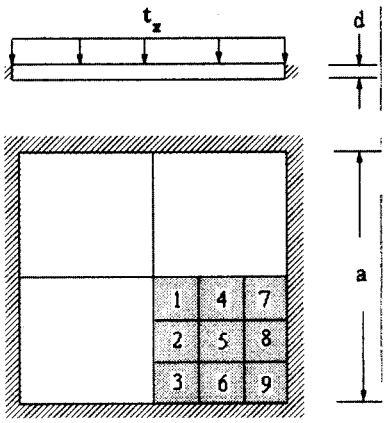

Fig. 2 A square plate-like structure subject to uniform normal traction ($a/d = 20$)

*This program was developed by the author during Ph.D. course at the Texas Institute for Computational and Applied Mathematics (TICAM) at the University of Texas at Austin.

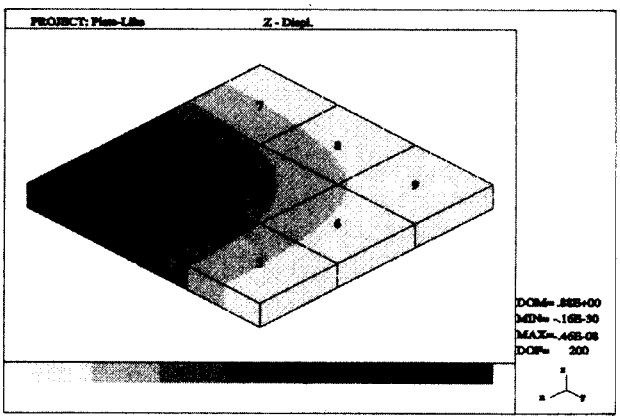

Fig. 3 Spectral distribution of vertical displacement component ($p=2$, $q=(1, 1, 0)^*$)

$$\theta=\left\{\sum_{K=1}^{N(\mathcal{P})}(\theta_K)^2\right\}^{1/2} \approx \| \hat{\boldsymbol{u}}_K^h - \boldsymbol{u}^{q,h} \|_{E(\Omega)} / \| \boldsymbol{u}_{\text{ref}} - \boldsymbol{u}^{q,h} \|_{E(\Omega)} \tag{59}$$

Table 1 contains the estimated results of the local and global error indicators and effectivity indices, and it shows comparison with the conventional error estimator which simply splits the interelement fluxes by half ($\alpha_{KL}=1/2$). Numerical results show that local error indices of the proposed method are considerably improved and more evenly distributed.

Next, we consider a cylindrical roof supported by two diaphragms, a representative engineering example, as shown in Fig. 4. By a diaphragm support is meant $u_r=u_\theta=0$, and loading is its own weight γ. The same material with the previous plate-like body is selected, and the other data are $L=5$ m, $R=1$ m, and $\gamma=4.0$ N/m^3. Using the symmetry of the body, numerical analysis was done by applying the (1, 1, 0)* -hierarchical model and 9 uniform quadratic elements to a quarter.

Fig. 5 depicts the distribution of radial displacement component, where we observe, from the value 8.6% of "DOM", that this problem is not bending-dominated. And since the radial displacement component is opposite to the radial direction, its magnitude is negative in the figure.

Following the same procedure for the estimate error indicators and effectivity indices, we obtain

Table 1 Estimated error and effectivity indices for the plate-like structure ($p=2$, $q=(1, 1, 0)^*$)

Elem No.	Error (E-7)			Effectivity Index	
	True	With Equil.	Without Equil.	With Equil.	Without Equil.
1	0.85307	0.87095	0.88607	1.02096	1.03868
2	0.53854	0.66702	0.81643	1.23855	1.51599
3	0.97427	0.99747	1.04193	1.02381	1.06944
4	0.53854	0.66702	0.81643	1.23855	1.51599
5	0.35162	0.54995	0.70580	1.56403	2.00726
6	0.66379	0.64317	0.75346	0.96894	1.13509
7	0.97427	0.99747	1.04193	1.02381	1.06944
8	0.66379	0.64317	0.75346	0.96894	1.13509
9	0.35837	0.31199	0.38437	0.87059	1.07255
Total	2.08314	2.20576	2.46389	1.05886	1.18278

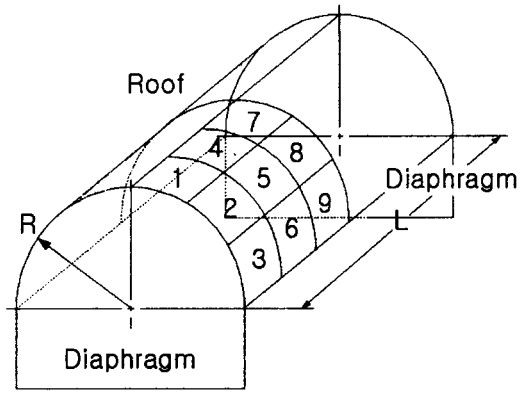

Fig. 4 A cylindrical roof supported by vertical diaphragms ($R/d = 20$)

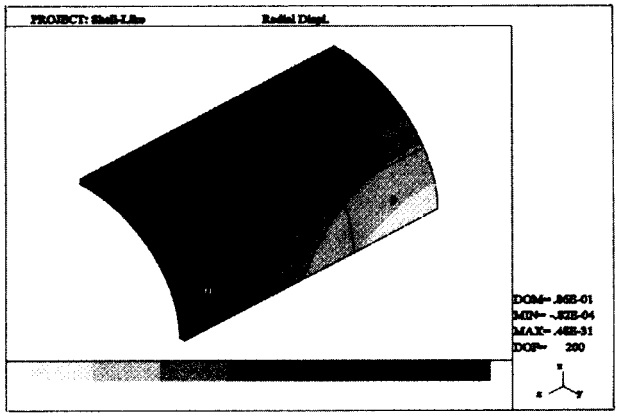

Fig. 5 Spectral distribution of radial displacement component (p=2, q=(1, 1, 0)*)

the numerical results recorded in Table 2. We see the improvement in the shell-like problems, too. In particular, big deviation in the conventional method is reported in the elements 5 and 8, while acceptable values are obtained with the proposed method.

Fig. 6 shows a distribution of local relative errors obtained by the proposed method. Here, the

Table 2 Estimated error and effectivity index for shell-like structure ($p = 2$, $q = (1, 1, 0)$*)

Elem No.	Error (E-3)			Effectivity Index	
	True	With Equil.	Without Equil.	With Equil.	Without Equil.
1	0.31097	0.32848	0.46491	1.05630	1.49503
2	0.29901	0.37936	0.52926	1.26875	1.77007
3	0.43736	0.48229	0.48249	1.10273	1.10318
4	0.66185	0.75400	1.09591	1.13924	1.65583
5	0.43974	0.61942	1.07351	1.40861	2.44123
6	0.76130	0.67162	0.70302	0.88220	0.92345
7	0.86592	0.91143	1.35222	1.05256	1.56160
8	0.53236	0.53972	1.19800	1.01044	2.25037
9	0.95932	0.76257	0.81017	0.79490	0.84452
Total	1.88199	1.89454	2.73803	1.00666	1.45486

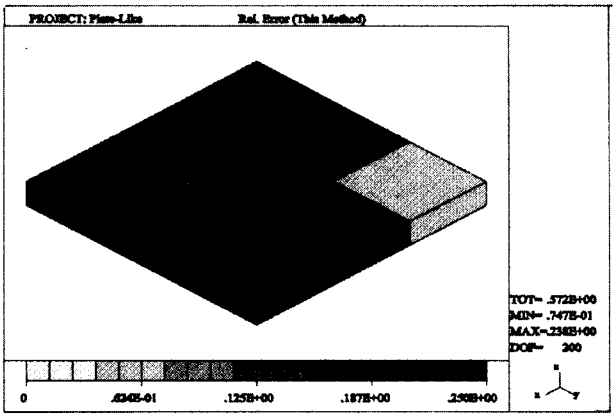

Fig. 6 Distribution of local relative errors ($p=2$, $q=(1,\ 1,\ 0)$*)

relative error is defined by $\eta_K^h / U(\boldsymbol{u}^{q,h})$. From the figure, the global relative error is 57.2% of total strain energy, and major contribution is come from the elements 1,3 and 7. It is interesting for the element 1 to have big error, however this phenomenon disappears when the (1, 1, 2)-hierarchical model, the next higher model by one level, is used, as shown in Fig. 7.

Figs. 8 and 9 represent distribution of local relative errors when the (1,1,0)*- and the (2,2,2)-hierarchical models, respectively, are employed for the approximation. A decrease in the global relative error from 54.5% to 44.5% indicates that the proposed error estimator successfully measures the modeling error component.

Table 3 contains the estimated global effectivity indices for different models and approximation orders for the plate-like problem. In particular, the plate-like problem is bending-dominated so locking phenomenon prevails when the finite-element approximation space is poor (Cho and Oden 1997).

However, from the data given in table, a quality of the proposed estimator does not deteriorate even at low approximation order, and this is because the reference solution $\hat{\boldsymbol{u}}_K^q$ is obtained using higher approximation order p_K^* on each local element-wise problem. For the numerical experiments, $\delta p=1$ (but, $\delta p=3$ for the initial $p_K=1$ to ensure upper bound against locking) and $\delta q=3$ (to

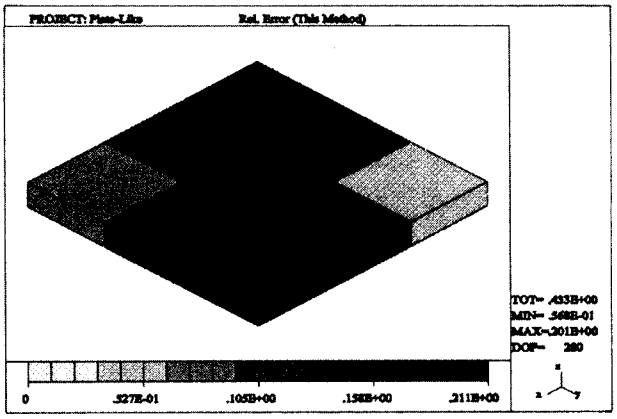

Fig. 7 Distribution of local relative errors ($p=2$, $q=(1,\ 1,\ 2)$)

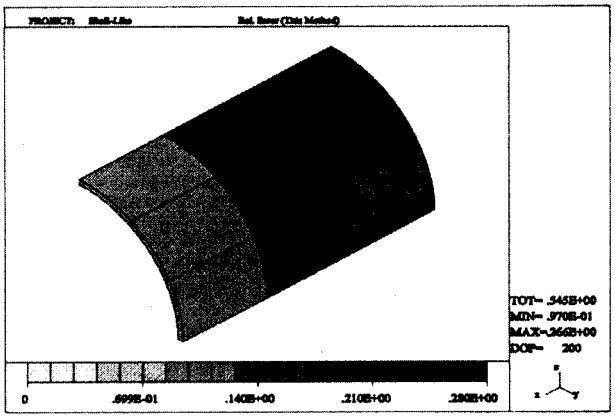

Fig. 8 Distribution of local relative errors (p=2, q=(1, 1, 0)*)

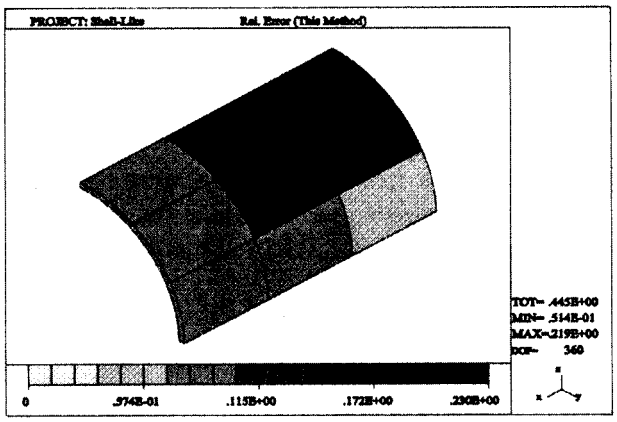

Fig. 9 Distribution of local relative errors (p = 2, q = (2, 2, 2))

Table 3 A variation of global effectivity indices for the plate-like structure

Approximation Order	Global effectivity indices			
	(1,1,0)*	(1,1,2)	(3,3,2)	(3,3,4)
p=1	1.118	1.131	1.101	1.102
p=2	1.059	1.078	1.038	1.041
p=3	1.001	1.055	1.064	1.150
p=4	1.001	1.034	1.014	1.051

sufficiently capture the boundary layer singularity near the boundary) are used. In addition, it is observed that the estimated global effectivity indices are stable with respect to a change of model levels, as listed in Table 3.

6. Conclusions and discussion

In this paper, with a brief introduction of the concept of hierarchical models, we derived an *a posteriori* error estimator for the hierarchical models for elastic structures with thin domains such

as plate- and shell-like structures, which can measure the total error with respect to the three-dimensional linear elasticity theory. In order to derive the proposed error estimator, the flux-splitting technique for element-wise force equilibrium and Lagrange multiplier method are employed. In order to approximate the exact solution, we use the self-equilibrated interelement tractions and solve the localized finite element problems with higher model levels and higher approximation orders.

From the two representative model problems, theoretical arguments underlying the error estimator have been verified. Compared to the conventional error estimator which splits interelement fluxes by half, better effectivity indices uniformly distributed over the elements are posssible.

Furthermore, since we use higher order enrichment p_K^* to solve the localized problems for $\hat{\boldsymbol{u}}_K^h$, a quality of this error estimator does not deteriorate when the finite element approximate solution $\boldsymbol{u}^{q,h}$ is suffered from locking phenomenon which may happen in standard finite element schemes with relatively coarse mesh and low approximation order.

With this tool, the analyst can estimate his numerical quality, and further he can control model levels, mesh sizes and approximation orders in order to enhance the accuracy together with the quality assurance and time saving.

Here, a question is: "*Can we apply the same theoretical results to other types of hierarchical models with different key parameters being used to determine the model level?*". Among other types of problems are two-phase composite bodies, general fluid flows, elasto-plastic behavior of inelastic bodies, however there has not been considerable advances on these fields. In order to extend the concept of hierarchical modeling, one should be able to construct the hierarchical family with a suitable key parameter and to obtain the solution corresponding to the highest model in such extended problems.

Acknowledgments

The financial support by Korea Science and Engineering Foundation under Grant No. 981-1002-016-2 is gratefully acknowledged.

References

Adams, R.A. (1978), Sobolev Spaces, Academic Press Inc.

Ainsworth, M. and Oden, J.T. (1993), "A unified approach to *a posteriori* error estimation using element residual methods", *Numer. Math.*, **65**, 23-50.

Babuska, I. and Li, L. (1992), "The problem of plate modeling: Theoretical and computational results", *Comp. Methods Appl. Mech. Engrg.*, **100**, 249-273.

Babuska, I., Szabo, B.A. and Actis, R.L. (1992), "Hierarchical models for laminated composites", *Numer. Methods Engrg.*, **33**, 503-535.

Cho, J.R. and Oden, J.T. (1996), "A priori modeling error estimates of hierarchical models for elasticity problems for plate- and shell-like structures", *Mathl. Comput. Modelling*, **23**(10), 117-133.

Cho, J.R. and Oden, J.T. (1996), "A priori error estimations of hp-finite element approximations for hierarchical models of plate- and shell-Like structures", *Comp. Methods Appl. Mech.*, **132**, 135-177.

Cho, J.R. and Oden, J.T. (1997), "Locking and boundary layer in hierarchical models for thin elastic structures", *Comp. Methods Appl. Mech.*, **149**, 33-48.

Ciarlet, P.G. (1978), *The Finite Element Method for Elliptic Problems*, North-Holland, Amsterdam.

Noor, A.K. and Burton, W.S. and Peters, J.M. (1992), "Hierarchical adaptive modeling of structural

sandwiches and multilayered composite panels", A.K. Noor ed., AMD-157, ASME Publications, 47-67.

Oden, J.T. and Cho, J.R. (1996), "Adaptive hpq-finite element methods of hierarchical models for plate- and shell-like structures", *Comp. Methods Appl. Mech. Engrg.*, **136**, 317-345.

Oden, J.T., Demkowicz, L. and Westermann, T.A. (1989), "Towards a universal h-p adaptive finite element strategy, Part 2: *A posteriori* error estimation", *Comp. Methods Appl. Mech. Engrg.*, **77**, 113-180.

Schwab, C. (1996), "*A posteriori* modelling error estimation for hierarchic plate models", *Numer. Math.*, **74**(2), 221-259.

Szabo, B.A. and Babuska, I. (1991), *Finite Element Analysis*, John Wiley, N.Y..

Szabo, B.A. and Sahrmann, G.J. (1988), "Hierarchic plate and shell models based on p-extensions", *Numer. Methods Engrg.*, **26**, 1855-1881.

Vogelius, M. and Babuska, I. (1981), "On a dimensional reduction method, I: The optimal selection of basis functions", *Math. Comp.*, **37**(156), 361-384.

Wempner, G. (1973), *Mechanics of Solids with Applications to Thin Bodies*, McGraw-Hill.

Zienkiewicz, O.C. and Zhu, J.G. (1987), "A simple error estimator and adaptive procedure for practical engineering analysis", *Numer. Methods Engrg.*, **24**, 337-357.